REPORT DOCUMENTATION PAGE

AFRL-SR-BL-TR-98-

0557

1. AGENCY USE ONLY (Leave blank)

2. REPORT DATE: 7/15/98

3. REPORT TYPE AND DATES COVERED: Final Technical report 8/15/97-5/14/98

4. TITLE AND SUBTITLE: "High Frequency Electromagnetic Propagation/Scattering Codes"

5. FUNDING NUMBERS: F49620-97-C-0052

6. AUTHOR(S): Vladimir Rokhlin

7. PERFORMING ORGANIZATION NAME(S) AND ADDRESS(ES):
Fast Mathematical Algorithms & Hardware Corporation
1020 Sherman Avenue
Hamden,CT 06514-1337

8. PERFORMING ORGANIZATION REPORT NUMBER: 4

9. SPONSORING/MONITORING AGENCY NAME(S) AND ADDRESS(ES):
USAF/AFMC
Air Force Office of Scientific Research/NM
110 Duncan Avenue, Room B115
Bolling AFB, DC 20332-8050

10. SPONSORING/MONITORING AGENCY REPORT NUMBER

19980805 005

11. SUPPLEMENTARY NOTES

12a. DISTRIBUTION/AVAILABILITY STATEMENT: Distribution is unlimited; approved for public release

12b. DISTRIBUTION CODE

13. ABSTRACT (Maximum 200 words) "Report developed under STTR Contract"

Whenever band-limited signals are measured or generated, different distributions of a fixed number of receivers and transducers lead to very different resolutions. A closely related set of issues is encountered in the numerical solution of scattering problems; given a scatterer, one would like to find nodes on its surface leading to most efficient discretizations. During Phase I of the STTR project F49629-97-C-0052, we discovered (somewhat werendipitoulsy) that whenever band-limited signals are to be discretized, measured, or generated, the construction of optimal (in a very strong sense) configurations of nodes is a tractable problem. When the nodes are to located on a line or on a disk in R^2, the solution is a fairly straightforward consequence of classical results obtained by Slepian and his collaborators more than 30 years ago. The required numerical tools are quite efficient; the resulting discretizations are a dramatic improvement over the ones currently employed.

Construction of optimal discretizations of more complicated regions requires additional mathematical apparatus; such apparatus has been largely (though by no means completely) designed. Unfortunately, the numerical tools we have constructed are quite inefficient in this environment, which limits the size of regions on which we are currently able to treat effectively. We have applied for the Phase II of the STTR project to further develop such analytical and numerical tools, and to apply them both in the engineering and numerical environments.

14. SUBJECT TERMS: STTR, Phase I, discretization

15. NUMBER OF PAGES: 32

16. PRICE CODE

17. SECURITY CLASSIFICATION OF REPORT	18. SECURITY CLASSIFICATION OF THIS PAGE	19. SECURITY CLASSIFICATION OF ABSTRACT	20. LIMITATION OF ABSTRACT
N/A	N/A	N/A	UL

"High Frequency Electromagnetic Propagation/Scattering Codes"

Final Technical Report
July 15, 1998

Small Business Technology Transfer (STTR) Program (DOD)
DCMC Hartford

Topic No: AF97T001

Issued by USAF, AFMC
Air Force Office of Scientific Research under

Contract No: F49620-97-C-0052

F.M.A.& H. Corporation
1020 Sherman Avenue
Hamden, CT 06514
Eff. Date of Contract: 8/15/97

P.I.: Paolo Barbano, Res.Sci.
(203)248-8212
This report covers period:
8/15/97 - 5/14/98

"The views and conclusions contained in this document are those of the authors and should not be interpreted as representing the official policies, either expressed or implied, of the Small Business Technology Transfer (STTR) Program or the U.S. Government."

"Distribution is unlimited; approved for public release."

High-Frequency Electromagnetic Propagation/Scattering Codes

1 Introduction

Whenever band-limited signals are measured or generated, the locations of receivers or transducers have to be selected; it is well-known that different distributions lead to very different resolutions given a fixed number of receivers or transducers. A closely related set of issues is encountered in the numerical solution of scattering problems: given a scatterer, one would like to find nodes on its surface leading to most efficient discretizations.

During Phase I of the STTR project F49620-97-C-0052, we discovered (somewhat serendipitously) that whenever band-limited signals are to be discretized, measured, or generated, the construction of optimal (in a very strong sense) configurations of nodes is a tractable problem. When the nodes are to be located on a line or on a disk in $\mathbb{R}^2$, the solution is a fairly straightforward consequence of classical results obtained by Slepian and his collaborators more than 30 years ago. We have constructed the necessary numerical tools, which are quite efficient; the resulting discretizations are a dramatic improvement over the ones currently employed.

Construction of optimal configurations of nodes on more complicated regions requires additional mathematical apparatus; such apparatus has been largely (but by no means completely) designed. Unfortunately, the numerical tools we have constructed are quite inefficient in this environment, which limits the size of regions on which we are currently able to design optimal configurations by approximately three wavelength. Needless to say that this state of affairs is not satisfactory; we are currently working on improved (in terms of CPU time requirements) algorithms for the construction of such configurations.

At the present time, we are finalizing the first of a series of papers describing this work (this paper describes the one-dimensional version of the theory). We have filed a patent disclosure with Yale University (of which we are attaching a copy), and applied

for the Phase II of this STTR project. The present report describes the state of affairs as of the conclusion of Phase I, with an emphasis of the analytical and numerical (as opposed to the engineering) aspects of the situation. It should be kept in mind that the results discussed here are very recent, and our view of the field is changing constantly.

2 Background

When measurements are performed, it often happens that the signal to be measured is well approximated by linear combinations of oscillatory exponentials, i.e. functions of the form

$$\sum_{j=1}^{n} \alpha_j \cdot e^{i \cdot \lambda_j \cdot x} \tag{1}$$

in one dimension, of the form

$$\sum_{j=1}^{n} \alpha_j \cdot e^{i \cdot (\lambda_j \cdot x + \mu_j \cdot y)} \tag{2}$$

in two dimensions, and of the form

$$\sum_{j=1}^{n} \alpha_j \cdot e^{i \cdot (\lambda_j \cdot x + \mu_j \cdot y + \nu_j \cdot z)} \tag{3}$$

in three dimensions. In most cases, the signal is band-limited, i.e. there exist such real positive a that all $1 \leq j \leq n$,

$$| \lambda_j | \leq a \tag{4}$$

in one dimension,

$$\lambda_j^2 + \mu_j^2 \leq a^2 \tag{5}$$

in two dimensions, and

$$\lambda_j^2 + \mu_j^2 + \nu^2 \leq a^2, \tag{6}$$

in three dimensions.

As is well-known, most measurements of electromagnetic and acoustic data (especially at reasonably high frequencies) are of this form. Examples of such situations include geophone and hydrophone strings in geophysics, phased array antennae in radar systems, multiple transceivers in ultrasound imaging, and a number of other applications astrophysics, medical imaging, non-destructive testing, etc.

In this proposal, we describe a procedure for determining the optimal distribution of sources and receivers that maximizes accuracy and resolution in measuring band-limited data given a fixed number of receivers. Alternatively, the procedure can be used to determine the optimal distribution of receivers that will minimize their number given specified accuracy and resolution. We illustrate the procedure with several examples of optimal distributions of receivers on an interval (one-dimensional case), on the disk (two-dimensional case), and on the triangle (two-dimensional case).

Remark 2.1 Our procedure permits the design of optimal receiver distributions in arbitrary regions in one, two, and three dimensions. However, when the region in question is an interval, a disk, or a sphere, there exists an explicit formula for the locations of the receivers, in terms of zeroes of the Generalized Prolate Spheroidal Wave Functions. Somewhat more complicated, but still nearly analytical, schemes exist when the region is the triangle (in two dimensions), a tetrahedron (in three dimensions), and in several other cases. In order to avoid describing the numerical apparatus required in the general case, we restrict our examples to the cases where the problem can be solved explicitly (as opposed to an involved numerical procedure).

The analytical apparatus we use is closely related both to classical Gaussian quadratures and to the analysis of band-limited functions initiated in the classical works [1]-[4]. It results in optimal (in a very strong sense) choice for both source and receiver locations. While the construction is quite straightforward in one dimension (in this case, it is a remarkably simple corollary to [1], [2]), in higher dimensions it is complicated by

the fact that regions can be of various shapes. In practical measurements, the cases of the string, of the disk, of the square, and of the triangle appear to be most frequently encountered.

3 Outline of Theory In One Dimension

Given a real $a > 0$, we will be considering the operator $P_a : L^2[-1,1] \rightarrow L^2[-1,1]$ defined by the formula

$$P_a(\varphi)(x) = \int_{-1}^{1} e^{i \cdot a \cdot x \cdot t} \cdot \varphi(t) dt, \tag{7}$$

for any $\varphi \in L^2[-1,1]$; the image of L^2 under P_a will be denoted by X_a. As observed in [1], all eigenvalues $\lambda_0, \lambda_1, \lambda_2, \cdots$ of the operator P_a are distinct, and the corresponding eigenvectors are the appropriately chosen Prolate Spheroidal Wave functions.

The following theorem is a combination of several Lemmas from [1].

Theorem 3.1 *For any positive real a, the eigenfunctions $\psi_0, \psi_1, \cdots$, of the operator P_a constitute an orthonormal basis in X_a. The function ψ_j has exactly i zeroes on the interval $[-1,1]$, and for any positive integer n, the functions $\psi_0, \psi_1, \cdots, \psi_n$ constitute a Chebychev system on the interval $[-1,1]$.*

Assuming that $\lambda_0, \lambda_1, \lambda_2, \cdots$ are ordered so that $\mid \lambda_0 \mid > \mid \lambda_1 \mid > \mid \lambda_2 \mid > \cdots$, the even-numbered eigenvalues are purely real, and the odd-numbered ones are purely imaginary. The even-numbered eigenfunctions are even, the odd-numbered ones are odd, and the $j-th$ eigenfunction has exactly j roots on the interval $[-1,1]$.

Finally, for all sufficiently large i,

$$\mid \lambda_j \mid < e^{-j}. \tag{8}$$

Remark 3.1 The operator (7) and some of its generalizations have been studied in [1]-[5]; later, a systematic investigation of generalizations of (7) was undertaken in [7]-[9]. The investigations reported in [1]-[5] appear to have been motivated almost entirely by

considerations of Electrical Engineering; the work [7]-[9] seems to have been motivated predominantly by considerations of pure mathematics. Remarkably, implications of this mathematical apparatus in numerical analysis appear to have been overlooked.

In the interests of brevity, we will be referring to the eigenfunctions ψ_n of the operator (7) as Slepian functions, and to their roots as Slepian nodes; abusing the notation somewhat, we will retain this terminology while discussing higher-dimensional versions of the operator (7), its eigenvalues, and their roots.

We will denote by A^n the $n \times n$-matrix defined by the formula

$$A^n_{j,k} = \psi_{j+1}(x_k), \tag{9}$$

with $x_1, x_2, \cdots, x_n$ the roots of the function ψ_n on the interval $[-1, 1]$.

The following theorem (with extensions to higher dimensions) is the basis of the numerical techniques we have been developing recently; its proof is somewhat involved and will be reported in the paper currently in preparation.

Theorem 3.2 *Suppose that for a positive real a, $x_1, x_2, \cdots, x_n$ are the zeroes on the interval $[-1, 1]$ of the eigenfunction ψ_n of the operator (7), and λ_n is the eigenvalue of (7) corresponding to ψ_n. Then there exist positive real numbers $w_1, w_2, \cdots, w_n$ such that*

$$||(B^n)^T \cdot B^n - I|| < \mid \lambda_n \mid, \tag{10}$$

where the matrix B^n is defined by the formula

$$B^n_{j,k} = A^n_{j,k} \cdot w_k, \tag{11}$$

and I denotes the unity matrix. Furthermore, for any real $\beta \in [-2a, 2a]$,

$$\mid \sum_{j=1}^{n} w_j \cdot e^{i \cdot \beta \cdot x_j} - \int_{-1}^{1} e^{i \cdot \beta \cdot x} dx \mid < \mid \lambda_n \mid, \tag{12}$$

Remark 3.2 The statement of Theorem 3.2 can be viewed as an extension of Gaussian quadratures from polynomials to linear combinations of exponentials, and as a tool for the construction of interpolation schemes. Indeed, (7) implies that the nodes $x_1, x_2, \cdots, x_n$ and corresponding weights $w_1, w_2, \cdots, w_n$ integrate (to the precision $\mid \lambda_n \mid$) all functions of the form $e^{i \cdot \beta \cdot x_j}$, with $\beta \in [-2a, 2a]$. Obviously, the dimensionality of the space of such functions (to precision $\mid \lambda_n \mid$) is roughly $2 \cdot n$. In other words, we have an n-point quadrature with positive weights integrating accurately functions from a space of dimensionality (roughly) $2 \cdot n$.

Given a band-limited function f on the interval $[-1, 1]$ tabulated at the nodes $x_1, x_2, \cdots, x_n$, an expansion of f into a linear combination

$$f(x) = \sum_{j=0}^{n-1} \gamma_j \cdot \psi_j(x) \tag{13}$$

is easily accomplished via the formula

$$\gamma = (A^n)^{-1}(F), \tag{14}$$

with $\gamma = (\gamma_0, \gamma_1, \cdots, \gamma_{n-1})$, $F = (f(x_0), f(x_1), \cdots, f(x_{n-1}))$, two vectors in $\mathbb{R}^n$. Since the matrix B^n is nearly orthogonal (see (7)), the latter procedure is guaranteed to be stable and provides a tool for the interpolation of band-limited functions.

4 Outline of Theory in Two Dimensions

For an arbitrary real $a > 0$, we will denote by D_a the disk in R^2 of radius a with the center at the origin. Given a region Ω in $\mathbb{R}^2$, we will be considering the operator $P_a : L^2(D_a) \to L^2(\Omega)$ defined by the formula

$$P_a(\varphi)(x) = \int_{A_a} e^{i \cdot (t,x)} \cdot \varphi(t) dt, \tag{15}$$

for any $\varphi \in L^2(D_a)$; the image of $L^2(D_a)$ under P_a will be denoted by X_a. We will define the operator $B_a : L^2(\Omega) \to L^2(\Omega)$ by the formula

$$B_a = P_a^* P_a, \tag{16}$$

with P_a^* denoting the adjoint of P_a. A simple calculation shows that B_a is given explicitly by the formula

$$B_a(\varphi)(x) = \int_\Omega \frac{J_1(a \cdot ||x-t||)}{||x-t||} dt. \tag{17}$$

Obviously, B_a is a non-negative definite symmetric operator whose spectrum and eigenfunctions are determined by the region Ω and the parameter a. We will order the eigenvalues λ_i of the operator B_a so that $\lambda_0 \geq \lambda_1 \geq \lambda_2 \geq \cdots$ and denote by ψ_i the eigenfunction corresponding to the eigenvalue λ_i.

Clearly, the operator B_a is compact; furthermore, its spectrum decays exponentially. An investigation of some of the properties of the operators P_a, B_a can be found in [4]). Given a function $f \in X_a$, it can be represented in the form

$$f(x) = \sum_{j=1}^{\infty} f_j \cdot \psi_j(x), \tag{18}$$

with $f_0, f_{1,2}, \cdots$ a (unique) sequence of complex coefficients. In a very strong sense, an expansion of the form (18) is the most efficient way to represent a function $f \in X_a$; without discussing the definition of an optimal representation in detail, we refer the reader to the classical paper [4] for a detailed discussion of such issues.

For each pair (i,j) of positive integers such that $i \neq j$, we will denote by $R_{i,j}$ the subset of Ω consisting of all points $x \in \Omega$ such that

$$\begin{aligned} \psi_i(x) &= 0, \\ \psi_j(x) &= 0. \end{aligned} \tag{19}$$

It is easy to see that for any $i,j \leq 0$, the set $R_{i,j}$ consists of at most a finite number of points in Ω; for certain pairs i,j, the set $R_{i,j}$ is empty.

The following observation is the basis of the procedure. Its proof is involved, and will be published at a later date.

Observation 4.1 *Suppose that for some integer $k, l > 0$, the set $R_{i,j}$ consists of n points $x_1, x_2, \cdots, x_n$. Then there exist positive real numbers $w_1, w_2, \cdots, w_n$ such that*

$$|\sum_{j=1}^{n} w_j \cdot e^{i\cdot(c,x_j)} - \int_{\Omega} e^{i\cdot(c,x)} | < S(\Omega) \cdot max(|\lambda_k|, |\lambda_l|, |\lambda_n|), \tag{20}$$

with $S(\Omega)$ denoting the area of Ω), and c an arbitrary vector in $\mathbb{R}^2$ such that

$$||c|| < 2 \cdot a. \tag{21}$$

In other words, given two singular functions ψ_k, ψ_l corresponding to eigenvalues λ_k, λ_l, the common zeroes of ψ_k, ψ_l can be viewed as the nodes of a quadrature formula on Ω for functions of the form

$$e^{i\cdot(c,x)}, \tag{22}$$

for all c satisfying the inequality (21); all weights of the obtained quadrature formula are positive. For all such functions, the relative error of the obtained quadrature is less than $max(|\lambda_k|, |\lambda_l|, |\lambda_n|)$.

The following observation is obtained from the preceding one via standard techniques of approximation theory.

Observation 4.2 *Suppose that under the conditions specified in Observation 4.1, the complex $n \times n$-matrix A_n is defined by the formula*

$$A^n_{j,k} = \sqrt{w_k} \cdot \psi_{j+1}(x_k). \tag{23}$$

Then

$$||(A^n)^* \cdot A^n - I|| < S(\Omega) \cdot max(|\lambda_k|, |\lambda_l|, |\lambda_n|), \tag{24}$$

In other words, the matrix connecting the coefficients of the (trancated) expansion (18), with its its values at the points $x_1, x_2, \cdots, x_n$ is almost orthogonal, for sufficiently large k, l, n.

Figure 1

50 nodes discretizing 20-wavelength interval at 3 digits

5 Examples

In this section, we present three four examples of receiver distributions, two in one dimension and two in two dimensions.

5.1 Examples in One Dimension

Both examples in one dimension are of distributions of receivers on an interval of a line. In both cases, the length of the interval is 20λ. However, in the first case, the relative accuracy of the receivers is assumed to be $1.0E-3$, while in the second case the accuracy of receivers is assumed to be $1.0E-6$. Obviously, in the second case, higher density of receivers is needed, since the higher inherent sensitivity of receivers will permit them to "sense" the insufficient resolution better. In the first case (Figure 1), the required number of receivers is 50, or 1.25 times the minimum number of nodes required by the Nyquist theorem (at fewer than 2 points per wavelength, an error of 100% is possible). In the second case (Figure 2), the required number of receivers is 56, or 1.4 times the Nyquist minimum.

5.2 Disks in Two Dimensions

Here, we present two examples: discretization of a disk of radius 5 wavelengths to 3 digits, and discretization of the same disk to 6 digits. As can be seen in Figures 3, 4,

Figure 2

56 nodes discretizing 20-wavelength interval at 6 digits

the 5-digit discretization requires 677 nodes, and the 6-digit one requires 796 nodes. A simple calculation shows that in the first case, we expend about 8.62 nodes per square wavelength of the region being discretized (about 2.15 times the Nyquist minimum). In the second case, the corresponding number is 10.13 nodes per square wavelength (about 2.53 times the Nyquist minimum).

Remark 5.1 The algorithms we used to obtain results presented in Figures 1-4 are based on practically analytical formulae for the determination of the optimal nodes; these formulae are an immediate consequence of some of the results in [1]- [4]. The CPU time requirements of the obtained numerical schemes grow as the square of the length of the interval in one dimension (measured in the number of wavelengths), and as the square of the radios of the disk in two dimensions. For all practical purposes, arbitrarily large numbers of such nodes can be constructed at a trivial cost in CPU time.

On the other hand, the nodes in Figures 5-7 are obtained by a significant generalization of the results of [4]; the resulting algorithms are extremely inefficient (the cost grows as the 6-th power of the size of the triangle!). The situation is salvaged to a large extent by the fact that each configuration has to be constructed only once, so that large expenditure of the CPU time is often affordable. Still, triangles in Figures 5-7 are much smaller than the disk in Figures 3,4.

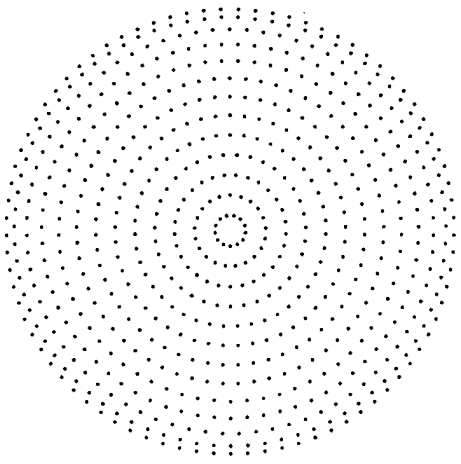

Figure 3

677 nodes discretizing to three digits a disk of radius 5 wavelengths

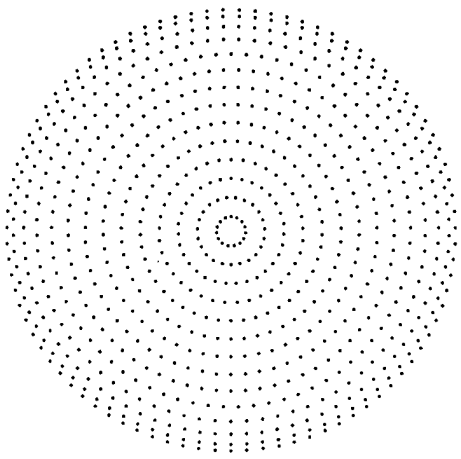

Figure 4

796 nodes discretizing to six digits a disk of radius 5 wavelengths

5.3 Triangles in Two Dimensions

Here, we present three examples: discretizations of an equilateral triangle with the side of length 1λ to 3 and 5 digits, and a discretization of an equilateral triangle with the side of length 2λ to 3 digits. As can be seen in Figures 5, 6, the 3-digit discretization requires 22 nodes, and the 6-digit one requires 40 nodes. The first case corresponds to about 51 nodes per square wavelength, and the second corresponds to about 92 nodes per square wavelength. A 3-digit discretization of a triangle with the side of length 2λ is depicted in In Figure 7. It requires 40 nodes, which ttranslates into about 23 nodes per square wavelength.

Remark 5.2 At first glance, it seems strange that the discretization in Figure 7 requires roughly twice as many nodes as that in Figure 6, while the area of the triangle is 4 times greater. However, this behavior is not at all anomalous, since for a sufficiently large region, the required number of nodes should converge to 4 points per square wavelength, as required by the Nyquist theorem. Generally, the required density of nodes increases with the decrease in the size of the region being discretized.

6 Application to the Measurements and Generation of Band-Limited Data

Due to the source-receiver duality in the antenna theory, we will be only discussing the applications of the techniques in the design of receiving antennae. The situation is identical in the design of radiating ones.

Assuming that our receivers are distributed on a specified region Ω in $\mathbb{R}^2$, and their sensitivity ε is specified, we would like to find the distribution of the receivers that would obtain the accuracy ε in the measurement of any function of the form (22), with $||c|| < a$.

Our procedure calls for constructing (numerically) the eigenvalues and eigenvectors of the operator B_a, and examining the common zeroes of several pairs of eigenvectors of B_a

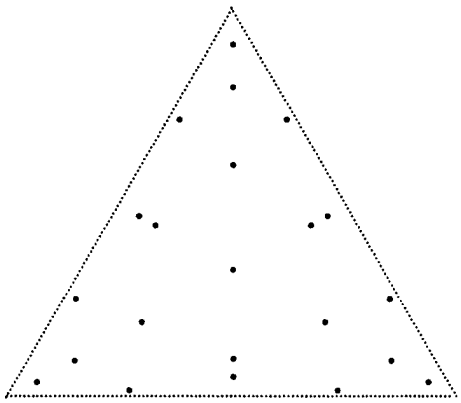

Figure 5

22 nodes discretizing to 3 digits an equilateral triangle with the side 1λ

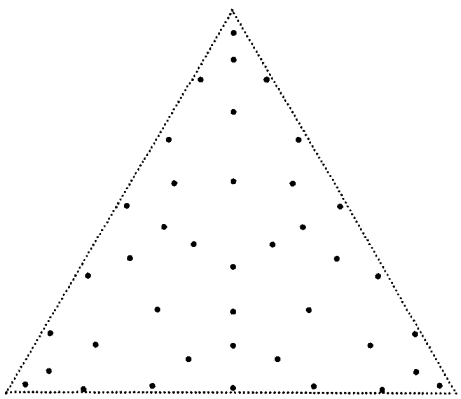

Figure 6

40 nodes discretizing to 5 digits an equilateral triangle with the side 1λ

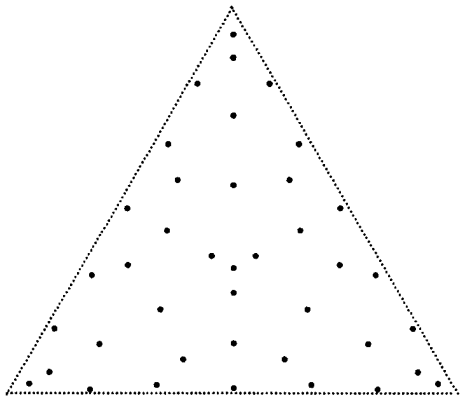

Figure 7

40 nodes discretizing to 3 digits an equilateral triangle with the side 2λ

whose corresponding eigenvalues are close to ε. Supposing that two such eigenfunctions ψ_k,ψ_l have n zeroes in common, and that $|\lambda_k| < \varepsilon$, $|\lambda_l| < \varepsilon$, $|\lambda_n| < \varepsilon$, the obtained nodes provide a satisfactory set of locations for the antennae. Choosing among such satisfactory sets the one for which n is minimized, we obtain the optimum distribution of antennae for the accuracy ε and region Ω.

Remark 6.1 Given a region in the plane (or on a surface in $\mathbb{R}^3$) where the phased array antenna is to be located, the analytical apparatus we have constructed provides (at some computational cost) optimal locations for the receivers or transducers. Clearly, this does not address the many engineering issues that will arize in connection with such configurations. At the present time, we are investigating these issues, while at the same time preparing a patent application for the procedure.

7 Application to the Discretization of Surfaces of Scatterers

When the technique is to be applied to the design of discretizations of surfaces of scatterers in the numerical modeling of electromagnetic and acoustic phenomena, we start with a triangulation of the surface. We will assume that the discretization provided to us satisfies the standard condition that the triangles on the surface have limited aspect ratios. It is usual to parametrize the triangles in a triangulation by the standard equilateral triangle in $\mathbb{R}^2$, and we assume that our triangles are so parametrized.

Given a user-specified accuracy and the size of the triangle on the surface (we measure the size in the number of wavelengths of the incoming radiation), we construct an optimum discretization of the standard triangle in the plane that guarantees the required precision *at a frequency somewhat higher than that at which the problem is being solved.* The actual amount of oversampling is determined by the smoothness of the surface in the region being discretized; most of the time, it will be determined predominantly by the quality of the CAD package that produced the surface being modeled. Now, the images on the surface of the scatterer of the nodes on the standard triangle are the nodes of the discretization of the surface. The associated quadrature and interpolation formulae on the standard triangle become (with appropriate scaling) the quadrature and interpolation formulae on the surface.

Remark 7.1 It should be observed that while the theory of such discretizations is quite straightforward (given the discretization of the standard triangle), we have only tested the resulting numerical procedure in two dimensions. Obviously, several numerical issues have to be resolved before the approach becomes an effective tool in the numerical solution of scattering problems in three dimensions.

References

[1] D. Slepian, H.O. Pollak, *Prolate Spheroidal Wave Functions, Fourier Analysis, and Uncertainty - I*, The Bell System Technical Journal, January 1961.

[2] H.J. Landau, H.O. Pollak, *Prolate Spheroidal Wave Functions, Fourier Analysis, and Uncertainty - II*, The Bell System Technical Journal, January 1961.

[3] H.J. Landau, H.O. Pollak, *Prolate Spheroidal Wave Functions, Fourier Analysis, and Uncertainty - III: The Dimension of Space of Essentially Time- and Band-Limited Signals*, The Bell System Technical Journal, July 1962.

[4] D. Slepian, *Prolate Spheroidal Wave Functions, Fourier Analysis, and Uncertainty - IV: Extensions to Many Dimensions, Generalized Prolate Spheroidal Wave Functions*, The Bell System Technical Journal, November 1964.

[5] D. Slepian, *Prolate Spheroidal Wave Functions, Fourier Analysis, and Uncertainty - V: The Discrete Case*, The Bell System Technical Journal, May-June 1978.

[6] D. Slepian, *Some Comments on Fourier Analysis, Uncertainty, and Modeling* SIAM Review, V. 25, No. 3, July 1983.

[7] F. A. Grünbaum, *Toeplitz Matrices Commuting With Tridiagonal Matrices*, J. Linear Alg. and Appl., 40, (1981).

[8] F. A. Grünbaum, *Eigenvectors of a Toeplitz Matrix: Discrete Version of the Prolate Spheroidal Wave Functions*, SIAM J. Alg. Disc. Meth., 2(1981).

[9] F. A. Grünbaum, L. Longhi, M. Perlstadt, *Differential Operators Commuting with Finite Convolution Integral Operators: Some Non-Abelian Examples*, SIAM J. Appl. Math. 42(1982).

A Procedure for the Design of Apparata for the Measurement of Band-Limited Signals

Abstract

Whenever physical signals are measured or generated, the locations of receivers or transducers have to be selected. Most of the time, this appears to be done on an ad hoc basis. For example, when a string of geophones is used in the measurements of seismic data in oil exploration, the receivers are located at equispaced points on an interval. When phased array antennae are constructed, their shapes are determined by certain aperture considerations; round and rectangular shapes are common. When antenna beams are steered electronically, it is done by changing the phases and the amplitudes of of the transducers. Again, these transducers are located in a region of predetermined geometry, and their actual locations within that geometry are chosen via some heuristic procedure.

In all these (and many other) cases, the signals being received or generated are *band-limited.* Optimal representation of such signals has been studied in detail in [1]-[4] more than 30 years ago. We use results from [1]-[4] (with some extensions) to construct optimal nodes for the measurement and generation of band-limited signals. In this disclosure, we describe the procedure based on these techniques for the design of such receiver (and transducer) configurations in a variety of environments.

1 Introduction

When measurements are performed, it often happens that the signal to be measured is well approximated by linear combinations of oscillatory exponentials, i.e. functions of the form

$$\sum_{j=1}^{n} \alpha_j \cdot e^{i \cdot \lambda_j \cdot x} \tag{1}$$

in one dimension, of the form

$$\sum_{j=1}^{n} \alpha_j \cdot e^{i\cdot(\lambda_j \cdot x + \mu_j \cdot y)} \tag{2}$$

in two dimensions, and of the form

$$\sum_{j=1}^{n} \alpha_j \cdot e^{i\cdot(\lambda_j \cdot x + \mu_j \cdot y + \nu_j \cdot z)} \tag{3}$$

in three dimensions. In most cases, the signal is band-limited, i.e. there exist such real positive a that all $1 \leq j \leq n$,

$$| \lambda_j | \leq a \tag{4}$$

in one dimension,

$$\lambda_j^2 + \mu_j^2 \leq a^2 \tag{5}$$

in two dimensions, and

$$\lambda_j^2 + \mu_j^2 + \nu^2 \leq a^2, \tag{6}$$

in three dimensions.

As is well-known, most measurements of electromagnetic and acoustic data (especially at reasonably high frequencies) are of this form. Examples of such situations include geophone and hydrophone strings in geophysics, phased array antennae in radar systems, multiple transceivers in ultrasound imaging, and a number of other applications in astrophysics, medical imaging, non-destructive testing, etc.

In this disclosure, we describe a procedure for determining the optimal distribution of sources and receivers that maximizes accuracy and resolution in measuring band-limited data given a fixed number of receivers. Alternatively, the procedure can be used to determine the optimal distribution of receivers that will minimize their number given specified accuracy and resolution. We illustrate the procedure with several examples of optimal distributions of receivers on an interval (one-dimensional case), on the disk (two-dimensional case), and on the triangle (two-dimensional case).

Remark 1.1 Our procedure permits the design of optimal receiver distributions in arbitrary regions in one, two, and three dimensions. However, when the region in question is an interval, a disk, or a sphere, there exists an explicit formula for the locations of the receivers, in terms of zeroes of the Generalized Prolate Spheroidal Wave Functions. Somewhat more complicated, but still nearly analytical, schemes exist when the region is the triangle (in two dimensions), a tetrahedron (in three dimensions), and in several other cases. In order to avoid describing the numerical apparatus required in the general case, we restrict our examples to the cases where the problem can be solved explicitly (as opposed to an involved numerical procedure).

The analytical apparatus we use is closely related both to classical Gaussian quadratures and to the analysis of band-limited functions initiated in the classical works [1]-[4]. It results in optimal (in a very strong sense) choice for both source and receiver locations. While the construction is quite straightforward in one dimension (in this case, it is a remarkably simple corollary to [1], [2]), in higher dimensions it is complicated by the fact that regions can be of various shapes. In practical measurements, the cases of the string, of the disk, of the square, and of the triangle appear to be most frequently encountered.

2 Outline of Theory In One Dimension

Given a real $a > 0$, we will be considering the operator $P_a : L^2[-1,1] \rightarrow L^2[-1,1]$ defined by the formula

$$P_a(\varphi)(x) = \int_{-1}^{1} e^{i \cdot a \cdot x \cdot t} \cdot \varphi(t) dt, \tag{7}$$

for any $\varphi \in L^2[-1,1]$; the image of L^2 under P_a will be denoted by X_a. As observed in [1], all eigenvalues $\lambda_0, \lambda_1, \lambda_2, \cdots$ of the operator P_a are distinct, and the corresponding eigenvectors are the appropriately chosen Prolate Spheroidal Wave functions.

The following theorem is a combination of several Lemmas from [1].

Theorem 2.1 *For any positive real a, the eigenfunctions* $\psi_0, \psi_1, \cdots$, *of the operator* P_a *constitute an orthonormal basis in* X_a. *The function* ψ_j *has exactly i zeroes on the interval* $[-1, 1]$, *and for any positive integer n, the functions* $\psi_0, \psi_1, \cdots, \psi_n$ *constitute a Chebychev system on the interval* $[-1, 1]$.

Assuming that $\lambda_0, \lambda_1, \lambda_2, \cdots$ *are ordered so that* $\mid \lambda_0 \mid > \mid \lambda_1 \mid > \mid \lambda_2 \mid > \cdots$, *the even-numbered eigenvalues are purely real, and the odd-numbered ones are purely imaginary. The even-numbered eigenfunctions are even, the odd-numbered ones are odd, and the* $j-th$ *eigenfunction has exactly* j *roots on the interval* $[-1, 1]$.

Finally, for all sufficiently large i,

$$\mid \lambda_j \mid < e^{-j}. \tag{8}$$

Remark 2.1 The operator (7) and some of its generalizations have been studied in [1]-[5]; later, a systematic investigation of generalizations of (7) was undertaken in [7]-[9]. The investigations reported in [1]-[5] appear to have been motivated almost entirely by considerations of Electrical Engineering; the work [7]-[9] seems to have been motivated predominantly by considerations of pure mathematics. Remarkably, implications of this mathematical apparatus in numerical analysis appear to have been overlooked.

In the interests of brevity, we will be referring to the eigenfunctions ψ_n of the operator (7) as Slepian functions, and to their roots as Slepian nodes; abusing the notation somewhat, we will retain this terminology while discussing higher-dimensional versions of the operator (7), its eigenvalues, and their roots.

We will denote by A^n the $n \times n$-matrix defined by the formula

$$A^n_{j,k} = \psi_{j+1}(x_k), \tag{9}$$

with $x_1, x_2, \cdots, x_n$ the roots of the function ψ_n on the interval $[-1, 1]$.

The following theorem (with extensions to higher dimensions) is the basis of the numerical techniques we have been developing recently; its proof is somewhat involved and will be reported in the paper currently in preparation.

Theorem 2.2 *Suppose that for a positive real a, $x_1, x_2, \cdots, x_n$ are the zeroes on the interval $[-1, 1]$ of the eigenfunction ψ_n of the operator (7), and λ_n is the eigenvalue of (7) corresponding to ψ_n. Then there exist positive real numbers $w_1, w_2, \cdots, w_n$ such that*

$$||(B^n)^T \cdot B^n - I|| < \mid \lambda_n \mid, \tag{10}$$

where the matrix B^n is defined by the formula

$$B^n_{j,k} = A^n_{j,k} \cdot w_k, \tag{11}$$

and I denotes the unity matrix. Furthermore, for any real $\beta \in [-2a, 2a]$,

$$\mid \sum_{j=1}^{n} w_j \cdot e^{i \cdot \beta \cdot x_j} - \int_{-1}^{1} e^{i \cdot \beta \cdot x} dx \mid < \mid \lambda_n \mid, \tag{12}$$

Remark 2.2 The statement of Theorem 2.2 can be viewed as an extension of Gaussian quadratures from polynomials to linear combinations of exponentials, and as a tool for the construction of interpolation schemes. Indeed, (7) implies that the nodes $x_1, x_2, \cdots, x_n$ and corresponding weights $w_1, w_2, \cdots, w_n$ integrate (to the precision $\mid \lambda_n \mid$) all functions of the form $e^{i \cdot \beta \cdot x_j}$, with $\beta \in [-2a, 2a]$. Obviously, the dimensionality of the space of such functions (to precision $\mid \lambda_n \mid$) is roughly $2 \cdot n$. In other words, we have an n-point quadrature with positive weights integrating accurately functions from a space of dimensionality (roughly) $2 \cdot n$.

Given a band-limited function f on the interval $[-1, 1]$ tabulated at the nodes $x_1, x_2, \cdots, x_n$, an expansion of f into a linear combination

$$f(x) = \sum_{j=0}^{n-1} \gamma_j \cdot \psi_j(x) \tag{13}$$

is easily accomplished via the formula

$$\gamma = (A^n)^{-1}(F), \tag{14}$$

with $\gamma = (\gamma_0, \gamma_1, \cdots, \gamma_{n-1})$, $F = (f(x_0), f(x_1), \cdots, f(x_{n-1}))$, two vectors in $\mathbb{R}^n$. Since the matrix B^n is nearly orthogonal (see (7)), the latter procedure is guaranteed to be stable and provides a tool for the interpolation of band-limited functions.

3 Outline of Theory in Two Dimensions

For an arbitrary real $a > 0$, we will denote by D_a the disk in R^2 of radius a with the center at the origin. Given a region Ω in $\mathbb{R}^2$, we will be considering the operator $P_a : L^2(D_a) \to L^2(\Omega)$ defined by the formula

$$P_a(\varphi)(x) = \int_{A_a} e^{i\cdot(t,x)} \cdot \varphi(t)dt, \tag{15}$$

for any $\varphi \in L^2(D_a)$; the image of $L^2(D_a)$ under P_a will be denoted by X_a. We will define the operator $B_a : L^2(\Omega) \to L^2(\Omega)$ by the formula

$$B_a = P_a^* P_a, \tag{16}$$

with P_a^* denoting the adjoint of P_a. A simple calculation shows that B_a is given explicitly by the formula

$$B_a(\varphi)(x) = \int_\Omega \frac{J_1(a \cdot ||x-t||)}{||x-t||} dt. \tag{17}$$

Obviously, B_a is a non-negative definite symmetric operator whose spectrum and eigenfunctions are determined by the region Ω and the parameter a. We will order the eigenvalues λ_i of the operator B_a so that $\lambda_0 \geq \lambda_1 \geq \lambda_2 \geq \cdots$ and denote by ψ_i the eigenfunction corresponding to the eigenvalue λ_i.

Clearly, the operator B_a is compact; furthermore, its spectrum decays exponentially. An investigation of some of the properties of the operators P_a, B_a can be found in [4]). Given a function $f \in X_a$, it can be represented in the form

$$f(x) = \sum_{j=1}^{\infty} f_j \cdot \psi_j(x), \tag{18}$$

with $f_0, f_{1,2}, \cdots$ a (unique) sequence of complex coefficients. In a very strong sense, an expansion of the form (18) is the most efficient way to represent a function $f \in X_a$; without discussing the definition of an optimal representation in detail, we refer the reader to the classical paper [4] for a detailed discussion of such issues.

For each pair (i,j) of positive integers such that $i \neq j$, we will denote by $R_{i,j}$ the subset of Ω consisting of all points $x \in \Omega$ such that

$$\begin{aligned} \psi_i(x) &= 0, \\ \psi_j(x) &= 0. \end{aligned} \tag{19}$$

It is easy to see that for any $i,j \leq 0$, the set $R_{i,j}$ consists of at most a finite number of points in Ω; for certain pairs i,j, the set $R_{i,j}$ is empty.

The following observation is the basis of the procedure being disclosed. Its proof is involved, and will be published at a later date.

Observation 3.1 *Suppose that for some integer $k,l > 0$, the set $R_{i,j}$ consists of n points $x_1, x_2, \cdots, x_n$. Then there exist positive real numbers $w_1, w_2, \cdots, w_n$ such that*

$$|\sum_{j=1}^{n} w_j \cdot e^{i\cdot(c,x_j)} - \int_{\Omega} e^{i\cdot(c,x)}| < S(\Omega) \cdot max(|\lambda_k|, |\lambda_l|, |\lambda_n|), \tag{20}$$

with $S(\Omega)$ denoting the area of Ω), and c an arbitrary vector in $\mathbb{R}^2$ such that

$$||c|| < 2 \cdot a. \tag{21}$$

In other words, given two singular functions ψ_k, ψ_l corresponding to eigenvalues λ_k, λ_l, the common zeroes of ψ_k, ψ_l can be viewed as the nodes of a quadrature formula on Ω for functions of the form

$$e^{i\cdot(c,x)}, \tag{22}$$

for all c satisfying the inequality (21); all weights of the obtained quadrature formula are positive. For all such functions, the relative error of the obtained quadrature is less than $max(|\lambda_k|, |\lambda_l|, |\lambda_n|)$.

The following observation is obtained from the preceding one via standard techniques of approximation theory.

Observation 3.2 *Suppose that under the conditions specified in Observation 3.1, the complex $n \times n$-matrix A_n is defined by the formula*

$$A^n_{j,k} = \sqrt{w}_k \cdot \psi_{j+1}(x_k). \tag{23}$$

Then

$$||(A^n)^* \cdot A^n - I|| < S(\Omega) \cdot max(|\lambda_k|, |\lambda_l|, |\lambda_n|), \tag{24}$$

In other words, the matrix connecting the coefficients of the (truncated) expansion (18), with its its values at the points $x_1, x_2, \cdots, x_n$ is almost orthogonal, for sufficiently large k, l, n.

4 Examples

In this section, we present three four examples of receiver distributions, two in one deimension and two in two dimensions.

4.1 Examples in One Dimension

Both examples in one dimension are of distributions of receivers on an interval of a line. In both cases, the length of the interval is 20λ. However, in the first case, the relative accuracy of the receivers is assumed to be $1.0E-3$, while in the second case the accuracy of receivers is assumed to be $1.0E-6$. Obviously, in the second case, higher density of receivers is needed, since the higher inherent sensitivity of receivers will permit them to "sense" the insufficient resolution better. In the first case (Figure 1), the required number of receivers is 50, or 1.25 times the minimum number of nodes required by the Nyquist theorem (at fewer than 2 points per wavelength, an error of 100% is possible). In the second case (Figure 2), the required number of receivers is 56, or 1.4 times the Nyquist minimum.

Figure 1

50 nodes discretizing 20-wavelength interval at 3 digits

Figure 2

56 nodes discretizing 20-wavelength interval at 6 digits

4.2 Disks in Two Dimensions

Here, we present two examples: discretization of a disk of radius 5 wavelengths to 3 digits, and discretization of the same disk to 6 digits. As can be seen in Figures 3, 4, the 5-digit discretization requires 677 nodes, and the 6-digit one requires 796 nodes. A simple calculation shows that in the first case, we expend about 8.62 nodes per square wavelength of the region being discretized (about 2.15 times the Nyquist minimum). In the second case, the corresponding number is 10.13 nodes per square wavelength (about 2.53 times the Nyquist minimum).

Remark 4.1 The algorithms we used to obtain results presented in Figures 1-4 are based on practically analytical formulae for the determination of the optimal nodes; these formulae are an immediate consequence of some of the results in [1]- [4]. The CPU time requirements of the obtained numerical schemes grow as the square of the length of the interval in one dimension (measured in the number of wavelengths), and as the square of the radios of the disk in two dimensions. For all practical purposes, arbitrarily large number oif such nodes can be construcrted at a trivial cost in CPU time.

On the other hand, the nodes in Figures 5-7 are obtained by a significant generalization of the results of [4]; the resulting algorithms are extremely inefficient (the cost grows as the 6-th power of the size of the triangle!). The situation is salvaged to a large extent by the fact that each configuration has to be constructed only once, so that large expenditure of the CPU time is often affordable. Still, triangles in Figures 5-7 are much smaller than the disk in Figures 3,4.

4.3 Triangles in Two Dimensions

Here, we present three examples: discretizations of an equilateral triangle with the side of length 1λ to 3 and 5 digits, and a discretization of an equilateral triangle with the side of length 2λ to 3 digits. As can be seen in Figures 5, 6, the 3-digit discretization

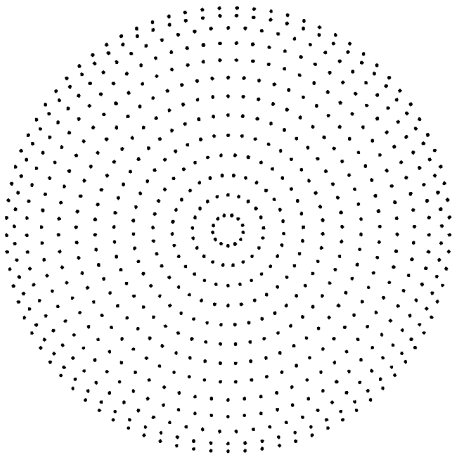

Figure 3

677 nodes discretizing to three digits a disk of radius 5 wavelengths

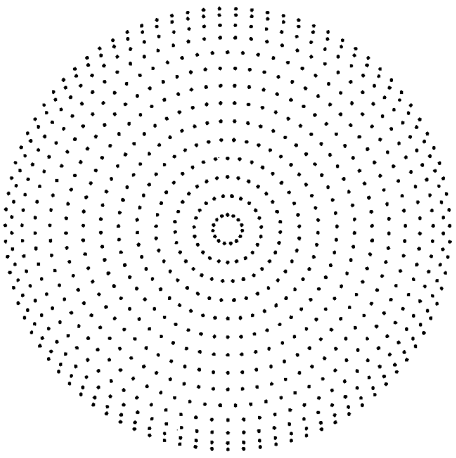

Figure 4

796 nodes discretizing to three digits a disk of radius 5 wavelengths

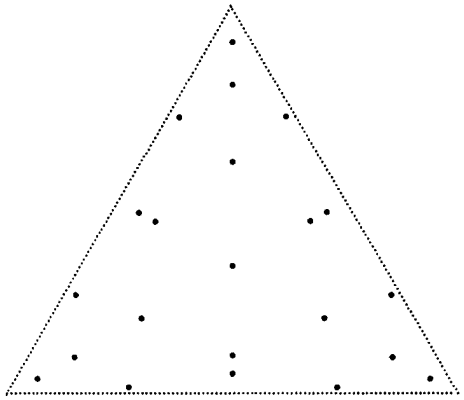

Figure 5

22 nodes discretizing to 3 digits an equilateral triangle with the side 1λ

requires 22 nodes, and the 6-digit one requires 40 nodes. The first case corresponds to about 51 nodes per square wavelength, and the second corresponds to about 92 nodes per square wavelength. A 3-digit discretization of a triangle with the side of length 2λ is depicted in In Figure 7. It requires 40 nodes, which translates into about 23 nodes per square wavelength.

Remark 4.2 At first glance, it seems strange that the discretization in Figure 7 requires roughly twice as many nodes as that in Figure 6, while the area of the triangle is 4 times greater. However, this behavior is not at all anomalous, since for a sufficiently large region, the required number of nodes should converge to 4 points per square wavelength, as required by the Nyquist theorem. Generally, the required density of nodes increases with the decrease in the size of the region being discretized.

5 Applications to the Measurements and Generation of Band-Limited Data

Due to the source-receiver duality in the antenna theory, we will be only discussing the applications of the techniques in the design of receiving antennae. The situation is

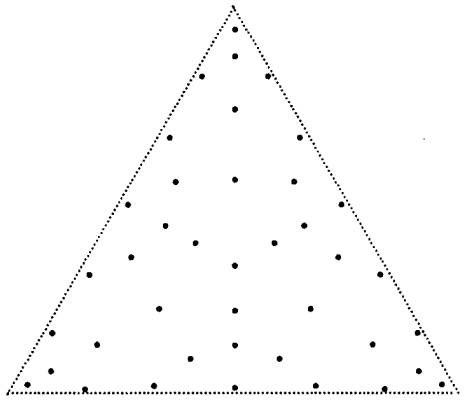

Figure 6

40 nodes discretizing to 5 digits an equilateral triangle with the side 1λ

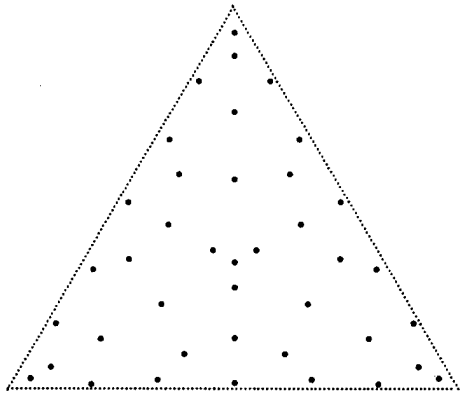

Figure 7

40 nodes discretizing to 3 digits an equilateral triangle with the side 2λ

identical in the design of radiating ones.

Assuming that our receivers are distributed on a specified region Ω in $\mathbb{R}^2$, and their sensitivity ε is specified, we would like to find the distribution of the receivers that would obtain the accuracy ε in the measurement of any function of the form (22), with $||c|| < a$.

Our procedure calls for constructing (numerically) the eigenvalues and eigenvectors of the operator B_a, and examining the common zeroes of several pairs of eigenvectors of B_a whose corresponding eigenvalues are close to ε. Supposing that two such eigenfunctions ψ_k,ψ_l have n zeroes in common, and that $|\lambda_k| < \varepsilon$, $|\lambda_l| < \varepsilon$, $|\lambda_n| < \varepsilon$, the obtained nodes provide a satisfactory set of locations for the antennae. Choosing among such satisfactory sets the one for which n is minimized, we obtain the optimum distribution of antennae for the accuracy ε and region Ω.

References

[1] D. Slepian, H.O. Pollak, *Prolate Spheroidal Wave Functions, Fourier Analysis, and Uncertainty - I*, The Bell System Technical Journal, January 1961.

[2] H.J. Landau, H.O. Pollak, *Prolate Spheroidal Wave Functions, Fourier Analysis, and Uncertainty - II*, The Bell System Technical Journal, January 1961.

[3] H.J. Landau, H.O. Pollak, *Prolate Spheroidal Wave Functions, Fourier Analysis, and Uncertainty - III: The Dimension of Space of Essentially Time- and Band-Limited Signals*, The Bell System Technical Journal, July 1962.

[4] D. Slepian, *Prolate Spheroidal Wave Functions, Fourier Analysis, and Uncertainty - IV: Extensions to Many Dimensions, Generalized Prolate Spheroidal Wave Functions*, The Bell System Technical Journal, November 1964.

[5] D. Slepian, *Prolate Spheroidal Wave Functions, Fourier Analysis, and Uncertainty - V: The Discrete Case*, The Bell System Technical Journal, May-June 1978.

[6] D. Slepian, *Some Comments on Fourier Analysis, Uncertainty, and Modeling* SIAM Review, V. 25, No. 3, July 1983.

[7] F. A. Grünbaum, *Toeplitz Matrices Commuting With Tridiagonal Matrices*, J. Linear Alg. and Appl., 40, (1981).

[8] F. A. Grünbaum, *Eigenvectors of a Toeplitz Matrix: Discrete Version of the Prolate Spheroidal Wave Functions*, SIAM J. Alg. Disc. Math., 2(1981).

[9] F. A. Grünbaum, L. Longhi, M. Perlstadt, *Differential Operators Commuting with Finite Convolution Integral Operators: Some Non-Abelian Examples*, SIAM J. Appl. Math. 42(1982).